

cdr

(Ba_{0.6}Sr_{0.4})TiO₃/PEEK composites modified by Polyethersulfone with low dielectric constant and high dielectric tunability under DC bias

Item Type	Article
Authors	Yang, Bin;Liu, Shuhang;Guo, Yiting;Hu, Guoxin;Wu, Sichen;Xu, Jie;Chen, Jianxin;Bulejak, Weronika;Baxter, Harry;Kong, Jie;Szafran, Mikołaj;Gao, Feng
Citation	Liu, S., Guo, Y., Hu, G., Wu, S., Xu, J., Chen, J., Bulejak, W., Baxter, H., Yang, B., Kong, J., Szafran, M., & Gao, F. (2023). (Ba _{0.6} Sr _{0.4})TiO ₃ /PEEK composites modified by Polyethersulfone with low dielectric constant and high dielectric tunability under DC bias. <i>Composites Science and Technology</i> , 233, 109929. https://doi.org/10.1016/j.compscitech.2023.109929
DOI	10.1016/j.compscitech.2023.109929
Publisher	Elsevier
Journal	Composites Science and Technology
Rights	Attribution-NonCommercial-NoDerivatives 4.0 International
Download date	2026-05-10 18:21:27
Item License	https://creativecommons.org/licenses/by-nc-nd/4.0/
Link to Item	http://hdl.handle.net/10034/627459

(Ba_{0.6}Sr_{0.4})TiO₃/PEEK composites modified by Polyethersulfone with low dielectric constant and high dielectric tunability under DC bias

Shuhang Liu¹, Yiting Guo¹, Guoxin Hu^{2*}, Sichen Wu¹, Jie Xu¹, Jianxin Chen^{3*}, Weronika Bulejak⁴,
Harry Baxter⁵, Bin Yang⁵, Jie Kong³, Mikołaj Szafran⁴, Feng Gao^{1*}

1 State Key Laboratory of Solidification Processing, MIIT Key Laboratory of Radiation Detection Materials and Devices, USI Institute of Intelligence Materials and Structure, NPU-QMUL Joint Research Institute of Advanced Materials and Structures (JRI-AMAS), School of Materials Science and Engineering, Northwestern Polytechnical University, 710072, Xi'an, Shaanxi, P. R. China

2 School of Materials Science and Engineering, Shaanxi Normal University, Xi'an 710119, P. R. China

3 Shaanxi Key Laboratory of Macromolecular Science and Technology, School of Chemistry and Chemical Engineering, Northwestern Polytechnical University, Xi'an, 710072, P. R. China

4 Faculty of Chemistry, Warsaw University of Technology, Noakowskiego 3, 00-664 Warsaw, Poland

5 Faculty of Science and Engineering, University of Chester, Parkgate Road, Chester, CH1 4BJ, United Kingdom

***Corresponding author:**

F. Gao, E-mail: gaofeng@nwpu.edu.cn

G.X. Hu, E-mail: huguoxin@snnu.edu.cn

J.X. Chen, E-mail: chenjianxin@nwpu.edu.cn

Abstract: Ceramic/polyetheretherketone (PEEK) composites show a wide range of applications and have attracted extensive interest in the scientific community due to their outstanding dielectric and mechanical characteristics. However, the interface connection between the ceramic and PEEK is a vital issue that must be addressed to improve their physical and electrical properties. In this work, the polyethersulfone resin (PES) was selected as interface modifier between barium strontium titanate (Ba_{0.6}Sr_{0.4}TiO₃, BST) and PEEK. Cold-pressing sintering was used to create BST/PEEK materials with superior dielectric frequency stability and dielectric tunability. The effects of PES content on the morphology and dielectric characteristics of PES modified BST/PEEK materials were investigated. The results showed PES could improve the dispersion of BST particles in polymer. The dielectric constant,

dielectric tunability, and breakdown strength increased first, then reduced as PES content increased. The composite had the most homogeneous microstructure and the best dielectric properties when the PES content was 7.5vol%. The frequency dispersion factor $F_{(x)}$ was much smaller than that of other ceramic/polymer composites reported. In addition, the dielectric tunability of the composites could reach a relatively high level (34.18%) while the dielectric constant was as low as 14. The dielectric tunable efficiency (T_{UE}) was proposed to evaluate the property of low dielectric constant and high dielectric tunability under DC bias. The T_{UE} of PES modified BST/PEEK composites show the highest value comparing with reported dielectric tunable composites. This research laid the path for the development of a novel ceramic/polymer composite with good interface bonding and high dielectric tunability.

Keywords: A. Polymer-matrix composites (PMCs); B. Dielectricity; B. Interface; E. Sintering

1 Instruction

Ceramic/polymer functional composites have the advantages of good flexibility, good machinability and light weight.^[1-4] In addition, its low processing temperature and simple process make it suitable for industrial electronic components and devices.^[5-7] Many compounds such as BaTiO₃^[8], SrTiO₃^[9], TiO₂^[10], (1-x)Pb(Mg_{1/3}Nb_{2/3})O₃-xPbTiO₃^[11, 12], KSr₂Nb₅O₁₅^[13] have been used as ceramics fillers to fabricate the ceramic/polymer functional composites.

Among them, Barium strontium titanate (Ba_{0.6}Sr_{0.4}TiO₃, BST), which shows special high dielectric tunability under DC bias, make it promising candidate material used for fabricating tunable capacitors and filters, tunable antennas, microwave phase shifters, etc.^[14-16] BST ceramics with great tunability, in general, have a high permittivity of 3500~4200.^[2] However, for practical applications of dielectric tunable devices, a low dielectric constant should be combined with great tunability, particularly in the microwave range.^[17] Additionally, BST ceramics have poor impact resistance and difficulty in manufacturing components with complex shapes, thus BST/polymer composite materials with proper dielectric constant, low dielectric loss and easy processing characteristics have attracted much attention in the past decade, such as BST/PVDF^[18], BST/ABS^[19], BST/PMMA^[20], BST/ABS-PVDF^[21], and BST/PEEK^[22], etc. BST/PEEK composite materials manufactured by cold-pressing sintering were recently described and shown the benefits of easy processing, high mechanical

characteristics, strong chemical stability, and steady dielectric constant with frequency variation. However, the structures of inorganic BST and organic matrix PEEK differ greatly^[23], and there is an obvious interface between BST fillers and PEEK matrix, leading to the breakdown of composite materials. Furthermore, due to PEEK's stable chemical properties and insolubility in most organic solvents, it is difficult to improve the interface bonding of BST/PEEK functional composites by surface treatment directly. It is necessary to find a new way to solve the problem of the interface connection between BST fillers and PEEK matrix, as well as keeping its dielectric properties and special dielectric tunability under DC bias.

Polyethersulfone (PES) is a high-performance amorphous polymer that can dissolve in a few polar solutions (such as N,N-Dimethylformamide, DMF)^[24] and has good binding property with BST inorganic particles^[25]. PES also has a molecular structure similar to that of PEEK, so an appropriate ratio of PES and PEEK has good compatibility and interface binding force.^[26] Researchers have carried out lots of work on the interface modification of inorganic/organic composites by PES, in order to improve the interface interaction between matrix and fillers and improve the comprehensive properties of composites. Wang et al.^[27] coated multi-walled carbon nanotubes with PES and then prepared MWCNTs/PEEK composites by melt extrusion method. The results showed that the composites could provide effective absorption shielding in 12~18 GHz band (Ku band) and 18~27 GHz band (K band). Ahmad et al.^[28] introduced sulfonated groups into the graphene/PES composite to enhance the interface bonding between PES and graphene, improve the dielectric constant and shielding effect of the materials, and reduce the leakage current of the composite with PES thin layer. Jiang et al.^[29] dispersed polyethersulfone (PES) coated graphite nanosheets (GNS) into polyether ether ketone (PEEK) matrix by melt blending to prepare wear-resistant composites with excellent tribological and mechanical/thermal properties.

At present, most studies about the PES surface modification are focused on improving hydrophilicity and friction coefficient, while few studies on dielectric properties of composites. Therefore, in order to further improve the interface bonding performance of BST/PEEK composite, PES was used as the buffer layer between BST and PEEK, and the influence of PES content on the microstructure and dielectric properties of BST/PEEK composite was studied to optimize the material composition. This work provides a new way to fabricate the composite materials with low dielectric constant and high dielectric tunability.

2 Experimental Methods

2.1 Processing of PES modified BST/PEEK composites

In this work, commercial BST ceramic powder, PES polymer powder and PEEK polymer powder were used as raw materials. **Figure 1** depicts the cold-pressing sintering method used to prepare the PES modified BST/PEEK functional composite material.

The first step was the modification of BST powder. Raw BST powders show amorphous morphology with average size of $\sim 1 \mu\text{m}$. A certain amount of PES powder was dissolved in 100 mL DMF solution and stirred magnetically for 30 min to form a homogeneous solution. Then, BST powder was added in proportion and stirred with magnetic force for 2 h, so that BST was evenly dispersed in PES DMF solution and BST suspension was obtained. The BST suspension was moved to the crucible and heated to 160°C on the heating stage in the fume hood to allow the DMF to evaporate. During the process, the solvent DMF was removed and PES was attached to the surface of BST powder to obtain the blended powder of BST and PES, which was labeled as PES-BST.

The second step was to prepare PES modified BST/PEEK composite material. PEEK powder was used as the matrix material and the PES-BST composite powder was used as the filling material. First, a certain volume ratio of PES-BST powder and PEEK powder was mixed in alcohol. The mixed powder was ground by ball for 12 h, and then dried. Then a green body with a radius of 6 mm and a thickness of 1 mm was prepared by dry pressing. The green body was sintered at 360°C and held for 1 h to obtain the final PES modified BST/PEEK composite material sample^[22], denoted as PES-BST/PEEK. The material composition is shown in **Table 1**. The samples with PES content of 2.5 vol%, 5.0 vol%, 7.5 vol% and 10.0 vol% were numbered PES-2.5, PES-5.0, PES-7.5 and PES-10.0, respectively.

2.2 Characterization

The phase composition of the produced PES-BST/PEEK composites was tested by X-ray diffraction (XRD, X'pert Pro MPD). The microstructure of the PES-BST/PEEK composites was examined using a scanning electron microscope (SEM, TESCAN VEGA3). The DSC214 and TA-SDT2960 differential scanning calorimeters from the German Neisch Company were used to perform thermogravimetric-differential thermal analysis (TG-DSC) on the PES-BST/PEEK functional composite at a heating rate of 10

K/min and estimate the glass transition temperature of the composite. The dielectric constant and loss were measured using an Agilent E4980A LCR meter (Palo Alto, CA). Furthermore, the breakdown voltages of PES-BST/PEEK functional composites were tested by using CJ2671S-type high voltage tester. And the composites' dielectric tunability was measured by the tunability testing system under DC bias at 1 kHz.

3. Results and Discussion

3.1 Microstructure of PES-BST composite powder

It is necessary to understand the microstructure of PES-BST composite powder before investigating the PES-BST/PEEK functional composites. **Figure 2(a)** shows the X-ray diffraction pattern of PES-BST powders. The PES-BST powders showed a clear perovskite structure, as shown in the figure, and the diffraction peak was compatible with the XRD standard card PDF#34-0411 of $\text{Ba}_{0.6}\text{Sr}_{0.4}\text{TiO}_3$. PES was an amorphous polymer so it was not shown in the XRD pattern. In addition, with the increase of PES content, the diffraction peaks of PES-BST powders gradually widened, indicating that the blending of PES and BST powder weakened the crystallinity of the composite powders.

The infrared spectrum of PES-BST powders is exhibited in **Figure 2(b)**. Compared with the standard spectrogram, it was found that there were characteristic peaks of benzene in the range of $1450\sim 1650\text{ cm}^{-1}$, and absorption peaks of sulfone group in the area of $1180\sim 1300\text{ cm}^{-1}$. The intensity of absorption peaks became higher and higher with the increase of PES content. This figure and the above XRD pattern together proved that the BST composite powders blended with PES were obtained.

3.2 Microstructure of PES-BST/PEEK composites

The X-ray diffraction patterns of PES-BST/PEEK functional composite materials are shown in **Figure 3**. The figure shows that PES-BST/PEEK functional composites were mostly perovskite phase, with no apparent polymer phase. PEEK is a semi-crystalline polymer material, and there is a wide semi-crystalline peak at $2\theta = 22^\circ$ in the XRD spectrum. PES is an amorphous polymer and was not shown in the XRD pattern. BST ceramic particles exhibited a perovskite structure, and the diffraction peak in **Figure 3** corresponded to the XRD standard card PDF#34-0411 of $\text{Ba}_{0.6}\text{Sr}_{0.4}\text{TiO}_3$.

Dense and uniform microstructure is very important to enhance the dielectric properties of ceramic/polymer functional composites. BST/PEEK composites without PES modification were prepared and the overall appearance of the composite material

was gray-brown with black spots on the surface, as shown in **Figure S1 (Supplementary Information)**. It can be seen that the mixing of BST and PEEK was not uniform, and the interface combination of BST and PEEK was poor for BST/PEEK composites without PES modification.

Figure 4 shows the scanning electron microscope photos of PES-BST/PEEK composite material. During the fabricating process, PEEK was cooled after melting and covered on the surface of PES-BST powder particles, forming a state of PEEK wrapping inorganic BST particles. The ceramic phase and polymer phase were evenly mixed and the surface contact was sufficient. As shown in **Figure 4(a)**, PEEK showed chain-like aggregation when PES content was low (red circle). This was because too few PES could not completely cover the BST surface, resulting in poor binding between PES-BST composite powder and PEEK. When the content of PES was too high (**Figure 4(d)**), the blended powder formed with BST was not uniform, which made the bonding between the composite powder PES-BST and PEEK worse, resulting in holes, cracks and other defects (yellow circle). Defects could weaken the interfacial bond of composites and easily generate interfacial charge.^[30] The accumulated interface charge will generate an offset electric field inside the material that is opposite to the external electric field, resulting in a smaller applied electric field on the composite material and a decrease in the internal polarization strength, which ultimately leads to a decrease in the PES-BST/PEEK functional composite material's dielectric characteristics. Therefore, PES modification with appropriate content can enhance the interfacial attachment of BST particles to the PEEK polymer matrix.

The glass transition point (T_g) and melting point (T_m) of the PES-BST/PEEK composite material were measured by thermal investigation utilizing differential scanning calorimetry (DSC) at a heating rate of 10 K/min. The results are shown in **Figure 5**. There were clear absorption/exothermic peaks with increasing temperature at 45°C, 150°C, and 350°C, corresponding to the sorption and release of N_2 , T_g , and T_m of the PES-BST/PEEK composites, respectively. The enlarged area in the figure was the T_g of the composite. **Table 2** lists the glass transition temperature and melting point of PES-BST/PEEK composite material. The glass transition temperature was the inflection point in the figure, and the melting point was the highest point of the endothermic peak.

In general, when a system formed by two partially mutually soluble liquids (e.g. A and B) reaches an equilibrium state at a certain temperature, two liquid phases co-exist.

One is a saturated solution of A in B, and the other is a saturated solution of B in A. The coexistence of these two saturated solutions is called a conjugate solution. The temperature at which the two conjugate solutions completely dissolve into one phase is called the critical solution temperature.^[31] For PEEK and PES systems, there is a similar phenomenon. If the system is conjugated, two glass transition temperatures can be measured in the system; if the system is completely miscible, only one glass transition occurs. Studies have shown that the critical dissolution temperature of PEEK and PES is 340°C^[32]. In this work, the sintering temperature of PES-BST/PEEK composite was 360°C, higher than the critical dissolution temperature of PEEK and PES, so only one glass transition phenomenon was observed in the figure. With the incremental PES content, the glass transition temperature of PES-BST/PEEK composite increased. This is because PES has a glass transition temperature of 225°C, which is higher than that of PEEK ($T_{g(PEEK)}=143^{\circ}\text{C}$). These values were consistent with the temperature correlating to the dielectric peak in the dielectric temperature spectrum of PES-BST/PEEK functional composite below, demonstrating that the sample's glass transition temperature would impact the material's dielectric characteristics.

As can be seen from **Figure 5**, bimodal melting peaks appeared near 350°C in the DSC curve of BST/PEEK composite without PES (black line). This is because PEEK material will recrystallize at this temperature when the crystallization time is sufficient, and the monomer difference in PEEK polymer is too large to form two kinds of mutually independent crystals.^[33] PES modification improved the melting characteristics of PEEK monomer polymer, so the bimodal melting peak disappeared. Furthermore, as PES is an amorphous polymer without a fixed melting point, the crystallization peak of the composite became wider with the increase of PES addition.

3.3 Dielectric properties of PES-BST/PEEK composites

Figure 6 shows the dielectric properties of PES-BST/PEEK functional composite material varying with frequency at room temperature. The test frequency was 100 Hz ~1M Hz. It can be seen that the permittivities of all samples decreased with the increase of frequency. The dielectric loss of PES-BST/PEEK composite decreased and the decreasing trend gradually slowed down with the incremental frequency. This was mainly caused by two polarization mechanisms in ceramic/polymer functional composites.^[34] When the frequency is low, the period of applied electric field is long enough to make the dipole orientation polarization and interface polarization response in the materials.^[35] When the frequency is high, the period of the external electric field

becomes shorter, so that the interface polarization of the composite material has no enough time to respond. At this time, the dielectric constant of the material mainly comes from the dipole orientation polarization, so the dielectric constant of the composites decreases. At 1k Hz, when PES volume fraction was 2.5 vol%, 5.0 vol%, 7.5 vol% and 10.0 vol%, the dielectric constants of the composites were about 13.5, 15.0, 14.2 and 8.9, respectively. With the increasing of PES content, the composites' dielectric constant increased first and then decreased. When PES volume fraction was 5.0 vol% and 7.5 vol%, the dielectric constants of the composites were higher. This indicated that the interfacial bonding of the composites sintered under this component was relatively good, which was consistent with the conclusion shown in the SEM photos above.

In order to measure the frequency stability of permittivity of ceramic/polymer composites, the $F_{(x)}$ (frequency dispersion factor) is defined as follows^[22]:

$$F_{(x)} = \frac{\varepsilon_{r(100)} - \varepsilon_{r(x)}}{\varepsilon_{r(100)}} \times 100\% \quad (1)$$

where $F_{(x)}$ is the composite's frequency dispersion factor and $\varepsilon_{r(100)}$ and $\varepsilon_{r(x)}$ are the composite's dielectric constants at 100 Hz and x Hz, respectively. The lower the value of $F_{(x)}$, the greater the dielectric frequency stability. $F_{(x)}$ is not available for optical frequencies. Most BST/polymer composites show $F_{(1M)}$ between 0.1 and 0.5048^[22]. $F_{(x)}$ of PES-BST/PEEK composite material with different PES contents was calculated, and the results are shown in **Figure 7**. The frequency dispersion factors of the composites increased with the increase of frequency. In the range of 100 Hz to 1M Hz, the frequency dispersion factors $F_{(1M)}$ of PES-BST/PEEK composite samples were all below 0.072, demonstrating that the composite's dielectric constant was frequency stable.

Figure 8 depicts the dielectric property curves of PES-BST/PEEK composite materials changing with temperature at 1k Hz. The test temperature was between 25°C and 200°C. The dielectric constant and dielectric loss of the composites with different PES contents generally increased with the increase of temperature, and there was a dielectric peak at 150°C. This is because the thermal motion of molecules is intensified with the increase of temperature, which makes the orientation polarization in the material easy to occur. When the temperature is near the T_g of the composites, the matrix material changes from the glass state to the viscoelastic state, and the degree of molecular thermal motion changes dramatically, resulting in an increase in the dielectric constant. The overall variation range of dielectric constant was small, and the dielectric

loss changed rapidly when the temperature was above 120°C, but was still less than 0.1. It indicates that the working temperature of PES-BST/PEEK composite materials can reach 200°C and this represents a higher level in polymer matrix composite materials, which benefits from the high heat resistance of PEEK matrix. At room temperature, when PES content was 2.5 vol%, 5.0 vol%, 7.5 vol% and 10.0 vol%, the dielectric constants of the composites were 13.5, 14.8, 14.1 and 8.9, accompanying with the low dielectric losses of 0.007, 0.016, 0.009 and 0.006, respectively.

Dielectric tunability is the property of a material in which the dielectric constant varies nonlinearly when the applied electric field changes, and its definition is shown in Equation (2)^[34]:

$$T_u = \frac{\varepsilon_{(0)} - \varepsilon_{(E)}}{\varepsilon_{(0)}} \times 100\% \quad (2)$$

where T_u represents the dielectric tunability, $\varepsilon_{(0)}$ and $\varepsilon_{(E)}$ represent the dielectric constant of the sample in the absence of external electric field and in the presence of external electric field respectively.

Figure 9 shows the variation curve of the dielectric tunability of PES-BST/PEEK composite under the applied DC bias electric field. As the figure shows, the dielectric tunability of PES-BST/PEEK composite increased with the rising of applied bias electric field. Besides, the dielectric tunability of PES-BST/PEEK composite rose slowly at first and then sharply with the incremental external electric field, and its mutation point is called threshold electric field.^[34] The dielectric tunability and threshold electric field of the samples with changing PES concentrations are listed in **Table 3**. It can be seen that with the increase of PES content, the dielectric tunability of the composite material increased first and then decreased, and the threshold electric field decreased. When PES content was 7.5 vol%, the dielectric tunability was 34.18% (at 6.5 kV/mm), and the threshold electric field was 1.0 kV/mm.

The degree of interfacial adhesion between the organic and inorganic phases influences the threshold electric field. The interface with better combination of ceramic and polymer has less hindrance to space charge and less charge accumulates at the interface, so the offset electric field generated by the charge at the interface becomes smaller and the actual electric field applied to the composite increases, which is helpful for the composite to achieve the rapid rise of dielectric tunability under the smaller external electric field. As can be seen from the above SEM pictures, PES-BST/PEEK functional composite with PES volume fraction of 7.5% has the best combination of inorganic phase and organic phase, so it shows the lowest threshold electric field and

the largest dielectric tunability.

The dielectric characteristics of PES-BST/PEEK samples are presented in **Table 3**. The dielectric properties of BST/PEEK composites without PES modification are given in the Supplementary Information file. The main problem of BST/PEEK composite was the poor combination of inorganic and organic materials, resulting in the low breakdown strength (11.15 kV/mm) of the composite, and its dielectric tunability was not high (8.75%), as shown in **Figure S2-S3**. It can be seen that when the volume fraction of PES was 2.5-10 vol%, the dielectric constants of the composite were 13.5, 15.0, 14.2 and 8.9, respectively, which were much higher than those of PEEK matrix (~3.2). At the same time, the dielectric tunability were ranging from 22.00% to 34.18%, the breakdown strength was increased to 41.37 kV/mm (**Figure S4**), which is much higher than that of BST/PEEK composites without PES modification. Through comparison, when PES content was 7.5vol %, the composite showed the best dielectric property.

Table 4 summarizes some of the dielectric characteristics of BST/polymer composites that have been reported. The dielectric constants of composites were in the range of 18~1250, the dielectric losses were in the range of 0.082 ~ 0.12, $F_{(IM)}$ was in the range of 0.061 ~ 0.773, the dielectric tunabilities were in the range of 3.36%~95.2%, and the breakdown strengths were between 46.7 kV/mm and 158.2 kV/mm. In this study, the dielectric loss of the PES-BST/PEEK composite (PES-7.5) was just 0.009, which was significantly lower than that of other composites. In addition, the value of $F_{(IM)}$ of PES-BST/PEEK composite was much smaller than that of other composites, indicating that the dielectric constant of PES-BST/PEEK composite had relatively small interface polarization loss with the increase of frequency, and had superior dielectric frequency stability.

As presented above, dielectrics with high tunability often exhibits a high permittivity^[2]. However, for practical applications of dielectric tunable devices, a low dielectric constant and strong tunability, particularly in the microwave region, are required^[17, 36]. Therefore, it is very essential that the BST/polymer composites have a proper dielectric constant and higher tunability. Compared with other composites, it is noticed that the dielectric tunability of PES-BST/PEEK composite could reach a relatively high level while its dielectric constant was low. In order to evaluate this characteristic, the dielectric tunable efficiency (T_{uE}) is proposed, as shown in Equation (3):

$$T_{uE} = \frac{T_u}{\varepsilon_r} \times 100\% \quad (3)$$

where T_u is the dielectric tunability of the composites, and ε_r is the relative dielectric constant of the material. The higher the T_{uE} is, the better the dielectric tunability of the composite is, and the more conducive to practical application. The T_{uE} of reported BST/polymer composites were shown in **Figure 10**. As can be seen, T_{uE} values of these composites were between 0.029% and 1.7%, while the dielectric tunable efficiency of PES-BST/PEEK composites (PES-7.5) amounts to 2.441%, showing obvious advantages. The high dielectric tunability with low dielectric constant of the PES-BST/PEEK composites is beneficial to the engineering applications of composite materials in integrated circuits and microwave dielectric devices^[37, 38].

3.4 Modification mechanism of PES-BST/PEEK composites

Figure 11 shows the modification mechanism of PES-BST/PEEK composites. In this experiment, BST is prone to agglomerate in polymer matrix, which leads to an inconsistent combination of the ceramic and polymer phases. PES powder was dissolved in DMF, and the long chain PES formed a network structure in DMF solvent. Then the BST was dissolved in DMF solution of PES. In the solution environment, the friction between BST particles was reduced, which was beneficial to improve the dispersion of BST. After removing the solvent DMF, the surface of BST was covered with a layer of PES molecules. This process is called the supersaturation mechanism.^[41, 42] When there are heterogeneous substances (BST), in the presence of heterogeneous material (BST), if the solvent (DMF) is reduced and the solution exceeds its supersaturation, there will be a large number of solute (PES) precipitation, attached to the surface of heterogeneous particles (BST). The interaction between BST and PES is physical adsorption. Next, the good compatibility between PES and PEEK improved the dispersion of BST particles in PEEK matrix. The molecular chains of PES and PEEK contain aromatic benzene ring structures. The weak interaction between these aromatic benzene ring structures, called π - π stacking^[43], makes PES and PEEK have good compatibility. π - π packing is usually found between two relatively electron-poor and electron-rich molecules, and is a non-covalent interaction similar to hydrogen bonding. There are three stacking modes: ①fully facing stack, ②partially facing stack, and ③facing edge stack, as shown in **Figure 11**. Therefore, PES served as a buffer layer between BST and PEEK, which was beneficial to enhance the interface binding of BST and PEEK, reduced the defects in microstructure, and obtained more superior dielectric properties. In the case of dielectric tunability, the reduction of defects at the

interface reduced the barrier effect of the interface on the charge, the internal counteracting electric field decreased, and the actual electric field on the material increased, which was conducive to the improvement of dielectric tunability. Generally to say, BST/PEEK functional composites with superior dielectric frequency stability and high dielectric tunability were obtained by enhanced interface connection between inorganic BST and PEEK matrix, which showed widely applications in processing tunable capacitors and filters, tunable antennas, microwave phase shifters, and other integrated electrical devices.

4 Conclusion

The PES-BST/PEEK functional composites were manufacture via cold-pressing sintering process. The introduction of PES increased the interface bonding between the ceramic and organic phases of the BST/PEEK composite, resulting in a relatively uniform microstructure and enhanced dielectric tunability. The PES-BST/PEEK composite demonstrated the most consistent morphology and the best dielectric characteristics when the PES component was 7.5 vol%: the dielectric constant was 14.2, the dielectric loss was 0.009, the dielectric tunability was 34.18% (1 kHz), the $F_{(1M)}$ was 0.051, and the dielectric tunability efficiency was 2.441%. Compared with other BST/polymer composites, PES-BST/PEEK composites have the advantages of low dielectric loss, good frequency stability and high dielectric tunability efficiency. This work paves the way for the synthesis of new ceramic/polymer composites with low dielectric constant and high dielectric tunability under DC bias.

Acknowledgement

This work was financially supported by the China-Poland International Collaboration Fund of National Natural Science Foundation of China (51961135301), the National Natural Science Foundation of China (52272123, 52072301), the ‘111’ Project (B20028), the Polish National Science Centre (No. 2018/30/Q/ST8/00205), the International Cooperation Foundation of Shaanxi Province (2022KW-34). We would like to thank the Analytical & Testing Center of Northwestern Polytechnical University for the measurements and valuable discussion of DSC, XRD, and SEM.

Reference

[1] J. Qiu, L. Weng, X. Zhang, et al., Sandwich-structured PPy-TiO₂/PVDF composite films with outstanding dielectric properties and energy density, J. IET Nanodielectrics. 5 (2022) 85-92,

<https://doi.org/10.1049/nde2.12031>.

- [2] F. Gao, K. Zhang, Y. Guo, et al., (Ba, Sr)TiO₃/polymer Dielectric composites---Progress and perspective, *J. Prog. Mater. Sci.* 121 (2021) 100813, <https://doi.org/10.1016/j.pmatsci.2021.100813>.
- [3] W. Xia, Z. Zhang, PVDF-based dielectric polymers and their applications in electronic materials, *J. IET Nanodielectrics*. 1(1) (2018) 17-31, <https://doi.org/10.1049/iet-nde.2018.0001>.
- [4] X.X. Yu, M.S. Xue, Z.Z. Yin, et al., Flexible boron nitride composite membranes with high thermal conductivity, low dielectric constant and facile mass production, *J. Compos. Sci. Technol.* (222) (2022) 109400, <https://doi.org/10.1016/j.compscitech.2022.109400>.
- [5] V.K. Palukuru, K. Sanoda, V. Pynttari, et al., Inkjet-printed RF structures on BST–polymer composites: an application of a monopole antenna for 2.4GHz wireless local area network operation, *INT J. Appl. Ceram. Tec.* 8(4) (2011) 940-946, <https://doi.org/10.1111/j.1744-7402.2010.02532.x>.
- [6] K. Nawaka, C. Putson, Enhanced electric field induced strain in electrostrictive polyurethane composites fibers with polyaniline (emeraldine salt) spider-web network, *J. Compos. Sci. Technol.* 198 (2020) 108293, <https://doi.org/10.1016/j.compscitech.2020.108293>.
- [7] J. Wenxu, H. Yudong, Z. Mupeng, et al., Advances in lead-free high-temperature dielectric materials for ceramic capacitor application, *J. IET Nanodielectrics*. 1(1) (2018) 3-16, <https://doi.org/10.1049/iet-nde.2017.0003>.
- [8] R. Zafar, N. Gupta, Dielectric characterisation of epoxy nanocomposite with barium titanate fillers, *J. IET Nanodielectrics*. 3 (2020) 53-61, <https://doi.org/10.1049/iet-nde.2019.0037>.
- [9] Z. Min, Y. Xi, S. Peng, et al., Effect of poly(vinyl acetate) on structure and property of bismuth-doped strontium titanate thin films derived by sol–gel method, *J. Ceram. Int.* 34(4) (2008) 997-1001, <https://doi.org/10.1016/j.ceramint.2007.09.066>.
- [10] A.R. Polu, R. Kumar, K.V. Kumar, et al., Effect of TiO₂ ceramic filler on PEG-based composite polymer electrolytes for magnesium batteries, *J. Am. J. Phys.* 1512 (2013) 996-997, <https://doi.org/10.1063/1.4791378>.
- [11] X. Zhuo, F. Chen, Z. Xi, et al., The studies of single crystal PMN-PT68/32/polymer 1–3 composites, *J. Ceram. Int.* 30 (2004) 1777-1780, <https://doi.org/10.1016/j.ceramint.2003.12.121>.
- [12] Z.H. Du, T.S. Zhang, M.M. Zhu, et al., Perovskite crystallization kinetics and dielectric properties of the PMN-PT films prepared by polymer-modified sol-gel processing, *J. J. Mater. Res.* 24(4) (2009) 1576-1584, <https://doi.org/10.1557/JMR.2009.0181>.
- [13] Y.T. Guo, G. Feng, X. Jie, et al., Fabrication and properties of (K_{0.52}Na_{0.48})NbO₃–KSr₂Nb₅O₁₅ lead-free ferroelectric composite ceramics, *J. J. Mater. Sci.-Mater. El.* 29 (2018) 12503-12511, <https://doi.org/10.1007/s10854-018-9369-5>.
- [14] Y. Li, G. Dong, Q. Liu, et al., Preparation and investigation on properties of BST-base ceramic with high-energy storage density, *J. J. Adv. Dielectr.* 3(1) (2013) 7.1-7.5, <https://doi.org/10.1142/S2010135X13500057>.
- [15] J. Cui, G. Dong, Z. Yang, et al., Low dielectric loss and enhanced tunable properties of Mn-doped BST/MgO composites, *J. J. Alloy. Compd.* 490(1) (2010) 353-357, <https://doi.org/10.1016/j.jallcom.2009.09.185>.
- [16] B. Vigneshwaran, P. Kuppasami, S. Ajithkumar, et al., Study of low temperature-dependent structural, dielectric, and ferroelectric properties of Ba_xSr_(1-x)TiO₃ (x = 0.5, 0.6, 0.7) ceramics, *J. J. Mater. Sci.-Mater. El.* 31(56) (2020) 10446-10459, <https://doi.org/10.1007/s10854-020-03593-3>.
- [17] V.O. Sherman, A.K. Tagantsev, N. Setter, Model of a low-permittivity and high-tunability ferroelectric based composite, *J. Appl. Phys. Lett.* 90(16) (2007) 989, <https://doi.org/10.1063/1.2723681>.

- [18] Y.T. Guo, S.H. Liu, S.C. Wu, et al., Enhanced dielectric tunable properties of BST/PVDF composites through dual-gradient structures, *J. J. Alloy. Compd.* 920 (2022) 166034, <https://doi.org/10.1016/j.jallcom.2022.166034>.
- [19] K.N. Zhang, F. Gao, J. Xu, et al., Fabrication and dielectric properties of Ba_{0.6}Sr_{0.4}TiO₃ / acrylonitrile–butadiene–styrene resin composites, *J. J. Mater. Sci.: Mater. El.* 28 (2017):8960-8968, <https://doi.org/10.1007/s10854-017-6626-y>.
- [20] X. Feng, W. Hong, K. Li, et al., Dielectric tunability of Ba_{0.6}Sr_{0.4}TiO₃/poly(methyl methacrylate) composites in 1-3-type structure, *J. Appl. Phys. Lett.* 91(19) (2007) 397, <https://doi.org/10.1063/1.2807845>.
- [21] Y.T. Guo, N. Meng, J. Xu, et al., Microstructure and dielectric properties of Ba_{0.6}Sr_{0.4}TiO₃/(acrylonitrile-butadiene-styrene)-poly(vinylidene fluoride) composites, *J. Adv. Compos. Hybrid Mater.* 2(4) (2019) 681-689, <https://doi.org/10.1007/s42114-019-00114-7>.
- [22] S.H. Liu, Y.T. Guo, J.W. Li, et al., Microstructure and dielectric properties of (Ba_{0.6}Sr_{0.4})TiO₃/PEEK functional composites prepared via cold-pressing sintering, *J. Compos. Sci. Technol.* 219 (2022) 109228, <https://doi.org/10.1016/j.compscitech.2021.109228>.
- [23] X. Zhang, Y. Ma, C. Zhao, et al., High dielectric constant and low dielectric loss hybrid nanocomposites fabricated with ferroelectric polymer matrix and BaTiO₃ nanofibers modified with perfluoroalkylsilane, *J. Appl. Surf. Sci.* 305 (2014) 531-538, <http://dx.doi.org/10.1016/j.apsusc.2014.03.131>.
- [24] Y. Hu, X. Hou, X. Hu, et al., Improvement in the mechanical and friction performance of poly(ether ether ketone) composites by addition of modificatory short carbon fibers and zinc oxide, *J. High Perform. Polym.* 30 (2017) 643-656, <https://doi.org/10.1177/0954008317723445>.
- [25] W. Xu, G. Yang, L. Jin, et al., High- k polymer nanocomposites filled with hyperbranched phthalocyanine-coated BaTiO₃ for high-temperature and elevated field applications, *J. ACS Appl. Mater. Interfaces.* 10 (2018) 11233-11241, <https://doi.org/10.1021/acsami.8b01129>.
- [26] B. Nandan, L.D. Kandpal, G.N. Mathur, Poly(ether ether ketone)/poly(aryl ether sulphone) blends: Thermal degradation behaviour, *J. Eur. Polym. J.* 39(1) (2003) 193-198, [https://doi.org/10.1016/S0014-3057\(02\)00170-2](https://doi.org/10.1016/S0014-3057(02)00170-2).
- [27] H. Wang, G. Wang, W. Li, et al., A material with high electromagnetic radiation shielding effectiveness fabricated using multi-walled carbon nanotubes wrapped with poly(ether sulfone) in a poly(ether ether ketone) matrix, *J. J. Mater. Chem.* 22(39) (2012) 21232-21237, <https://doi.org/10.1039/c2jm35129c>.
- [28] M.W. Ahmad, B. Dey, A.A. Sammar, et al., Sulfonic-functionalized graphene oxide reinforced polyethersulfone nanocomposites with enhanced dielectric permittivity and EMI shielding effectiveness, *J. J. Mater. Chem.* 39 (2012) 21232-21237, <https://doi.org/10.1039/c2jm35129c>.
- [29] W. Jiang, X. Jin, H. Zhang, et al., Poly(ether ether ketone)/wrapped graphite nanosheets with poly(ether sulfone) composites: Preparation, mechanical properties, and tribological behavior, *J. J. Appl. Polym. Sci.* 132(14) (2015) 41728, <https://doi.org/10.1002/app.41728>.
- [30] L. L. Wang, C.C. Liu, Z.X. Bai, et al., Superhydrophobic ZIF-8/PEN films with ultralow dielectric constant and outstanding mechanical properties, *J. Compos. Sci. Technol.* 225 (2022) 109498, <https://doi.org/10.1016/j.compscitech.2022.109498>.
- [31] H.G. Schild, D.A. Tirrell, Microcalorimetric detection of lower critical solution temperatures in aqueous polymer solutions, *J. J. Phys. Chem.* 94(10) (1990) 4352-4356, <https://doi.org/10.1021/j100373a088>.

- [32] X. Yu, Y. Zheng, Z. Wu, et al., Study on the compatibility of the blend of poly(aryl ether ether ketone) with poly(aryl ether sulfone), *J. J. Appl. Polym. Sci.* 41(11-12) (2010) 2649-2654, <https://doi.org/10.1002/app.1990.070411112>.
- [33] T. Kwon, J. Koo, H. Choi, Surface-mediated recrystallization for highly conducting organic radical crystal, *J. Cryst. Growth Des.* 19 (2019) 551–555, <https://doi.org/10.1021/acs.cgd.8b01686>.
- [34] Q.Q. Zhang, F. Gao, C.C. Zhang, et al., Enhanced dielectric tunability of Ba_{0.6}Sr_{0.4}TiO₃/Poly(vinylidene fluoride) composites via interface modification by silane coupling agent, *J. Compos. Sci. Technol.* 129 (2016) 93e100, <http://doi.org/10.1016/j.compscitech.2016.04.016>.
- [35] Z.X. Huang, M.L. Zhao, G.Z. Zhang, et al., Controlled localizing multi-wall carbon nanotubes in polyvinylidene fluoride/acrylonitrile butadiene styrene blends to achieve balanced dielectric constant and dielectric loss, *J. Compos. Sci. Technol.* 212(11) (2021) 108874, <https://doi.org/10.1016/j.compscitech.2021.108874>.
- [36] K. Zhou, S.A. Boggs, R. Ramprasad, et al., Dielectric response and tunability of a dielectric-paraelectric composite, *J. Appl. Phys. Lett.* 93(10) (2008) 325, <https://doi.org/10.1063/1.2982086>.
- [37] W. Rui, Z. Ji, L. Bo, et al., CaF₂-AlF₃-SiO₂ glass-ceramic with low dielectric constant for LTCC application, *J. J. Alloy. Compd.* 490 (2010) 204-207, <https://doi.org/10.1016/j.jallcom.2009.09.031>.
- [38] Y.Y. Fong, B. Subhash, Pure silica zeolite beta membrane: A potential low dielectric constant material for microprocessor application, *J. J. Appl. Sci.* 7(15) (2007), <https://doi.org/10.3923/jas.2007.2040.2045>.
- [39] Q.Q. Zhang, G. Feng, G.X. Hu, et al., Characterization and dielectric properties of modified Ba_{0.6}Sr_{0.4}TiO₃/poly(vinylidene fluoride) composites with high dielectric tunability, *J. Compos. Sci. Technol.* 118 (2015) 94-100, <http://dx.doi.org/10.1016/j.compscitech.2015.08.013>.
- [40] Y.T. Guo, N. Meng, Y. Zhang, et al., Characterization and performance of plate-like Ba_{0.6}Sr_{0.4}TiO₃/Poly(vinylidene fluoride -trifluoroethylene -chlorotrifluoroethylene) composites with high permittivity and low loss, *J. Polymer.* 203 (2020) 122777, <https://doi.org/10.1016/j.polymer.2020.122777>.
- [41] D. Kashchiev, G. Rosmalen, Nucleation in solutions revisited, *J. Cryst. Res. Technol.* 38(7-8) (2003) 555-574, <https://doi.org/10.1002/crat.200310070>.
- [42] M.Y. Yang, W. Gong, Y.L. Wang, et al. Bioavailability improvement strategies for poorly water-soluble drugs based on the supersaturation mechanism: An update, *J. J. Pharm. Sci-US* 19 (2016) 205-225, <https://doi.org/10.18433/J3W904>.
- [43] J. Bjork, F. Hanke, C.A. Palma, et al., Adsorption of aromatic and anti-aromatic systems on graphene through π - π stacking, *J. J. Phys. Chem. Lett.* 1(23) (2010) 3407, <https://doi.org/10.1021/jz101360k>.

Figure Captions

Figure 1 Preparation process of flow chart.

Figure 2 Phase structure and morphology of PES-BST powders, (a) XRD patterns, (b) infrared spectra.

Figure 3 XRD patterns of PES-BST/PEEK composites, (a) PES-2.5, (b) PES-5.0, (c) PES-7.5 and (d) PES-10.0.

Figure 4 SEM images of PES-BST/PEEK composites, (a) PES-2.5 (b) PES-5.0 (c) PES-7.5 and (d) PES-10.0.

Figure 5 Thermal analysis curves of PES-BST/PEEK composites, (a) DSC curves and (b) glass transition temperature region.

Figure 6 Frequency dependence of dielectric properties of PES-BST/PEEK composites.

Figure 7 The frequency dispersion factor of PES-BST/PEEK composites.

Figure 8 Temperature dependence of dielectric properties of PES-BST/PEEK composites at 1k Hz, (a) dielectric constant and (b) dielectric loss.

Figure 9 Dielectric tunability of PES-BST/PEEK composites.

Figure 10 Dielectric properties of BST/polymer composites.

Figure 11 Modification mechanism of PES-BST/PEEK composites.

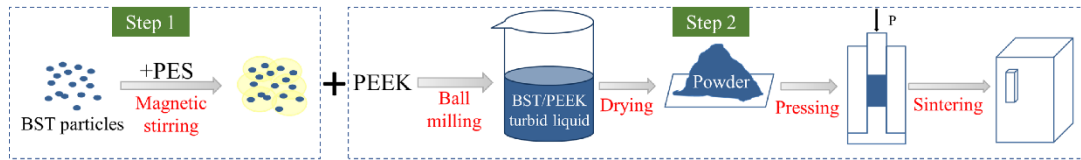


Fig. 1 Preparation process of flow chart.

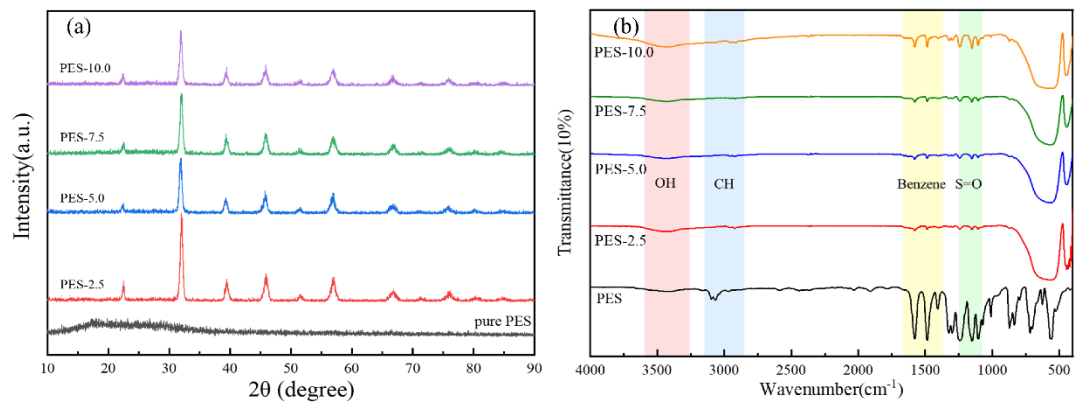


Fig. 2 Phase structure and morphology of PES-BST powders,

(a) XRD patterns, (b) infrared spectra

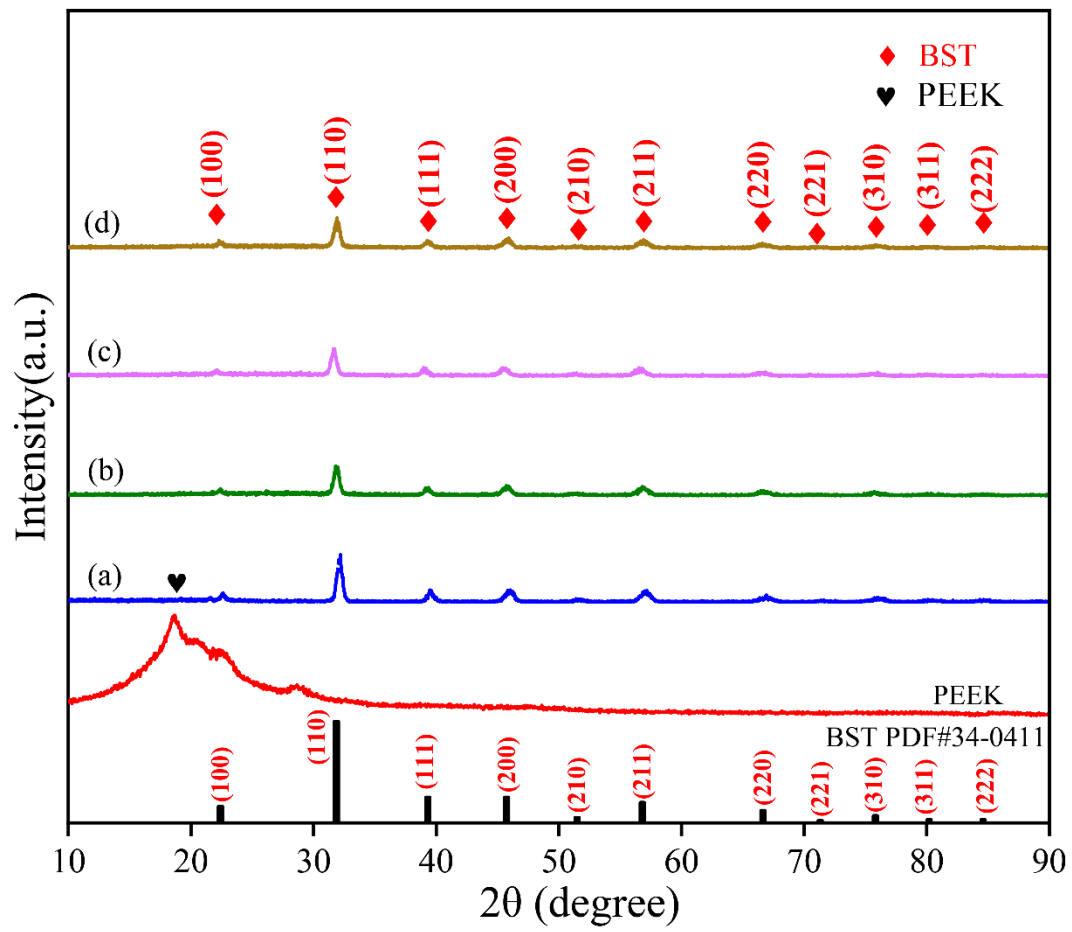


Fig. 3 XRD patterns of PES-BST/PEEK composites, (a) PES-2.5, (b) PES-5.0, (c) PES-7.5 and (d) PES-10.0.

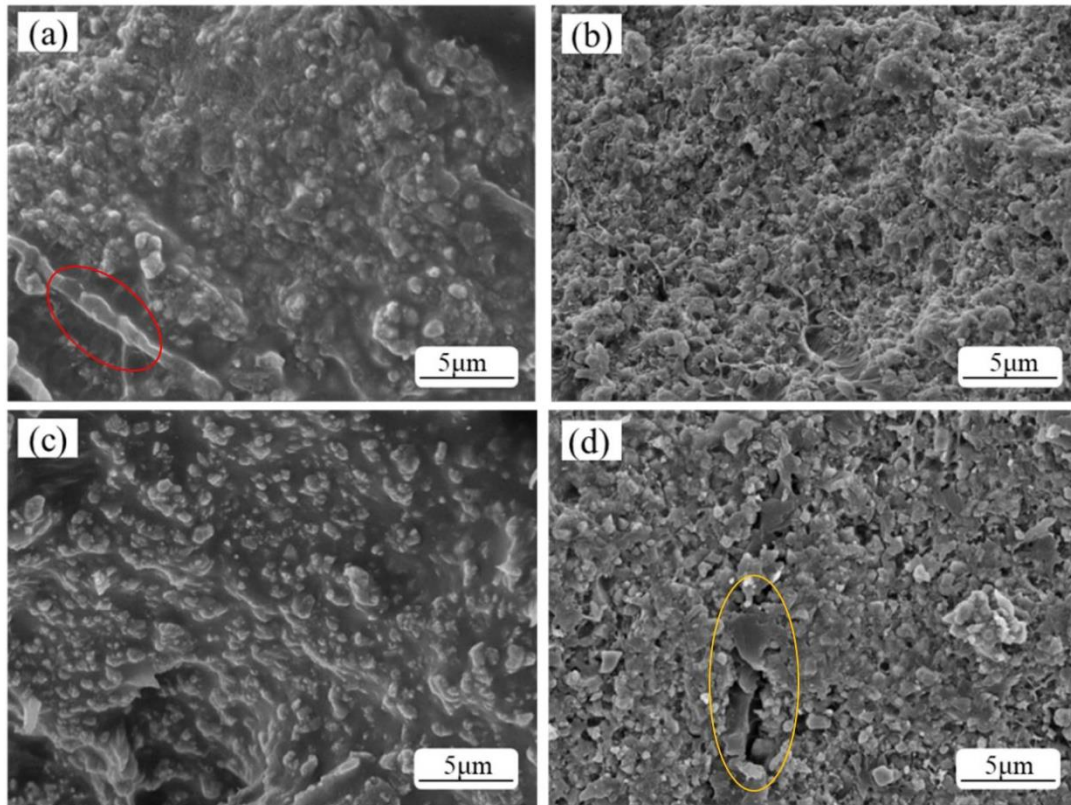


Fig. 4 SEM images of PES-BST/PEEK composites,
(a) PES-2.5 (b) PES-5.0 (c) PES-7.5 and (d) PES-10.0.

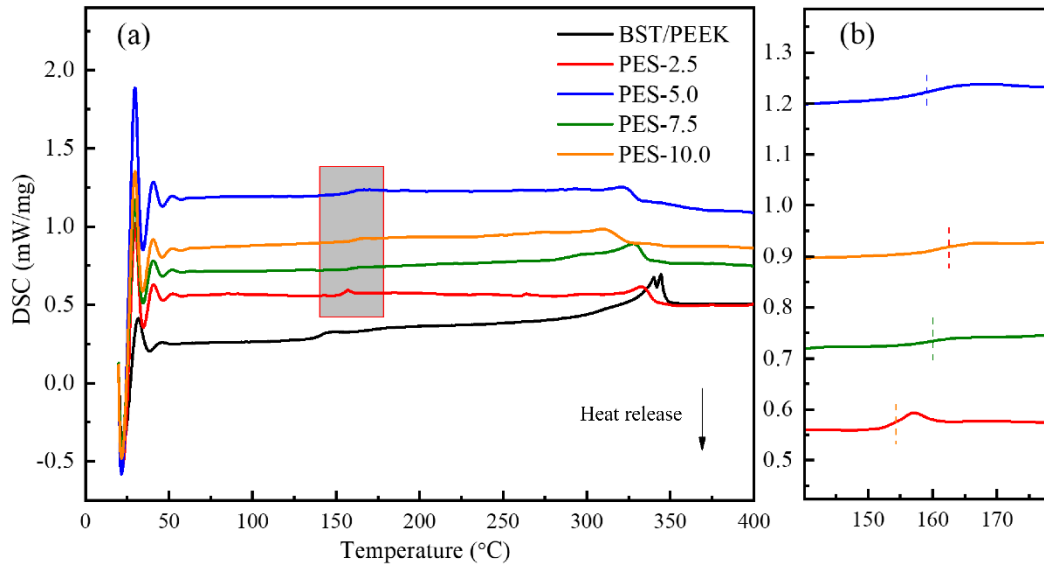


Fig. 5 Thermal analysis curves of PES-BST/PEEK composites, (a) DSC curves and (b) glass transition temperature region.

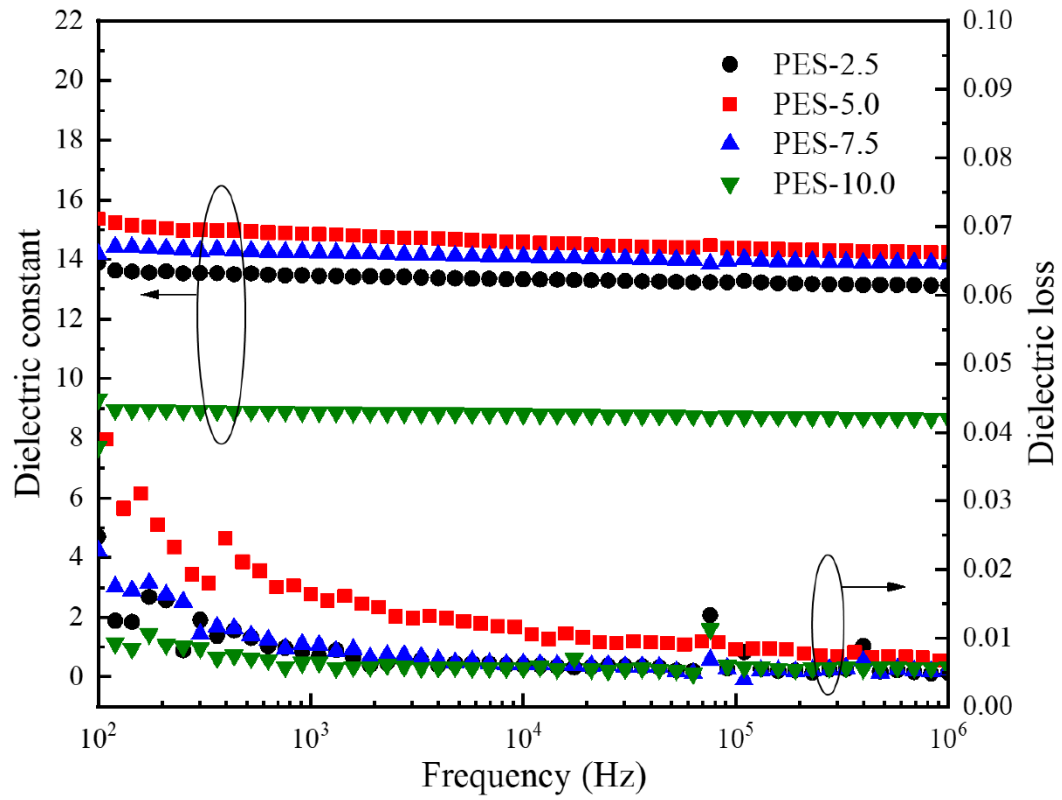


Fig. 6 Frequency dependence of dielectric properties of PES-BST/PEEK composites.

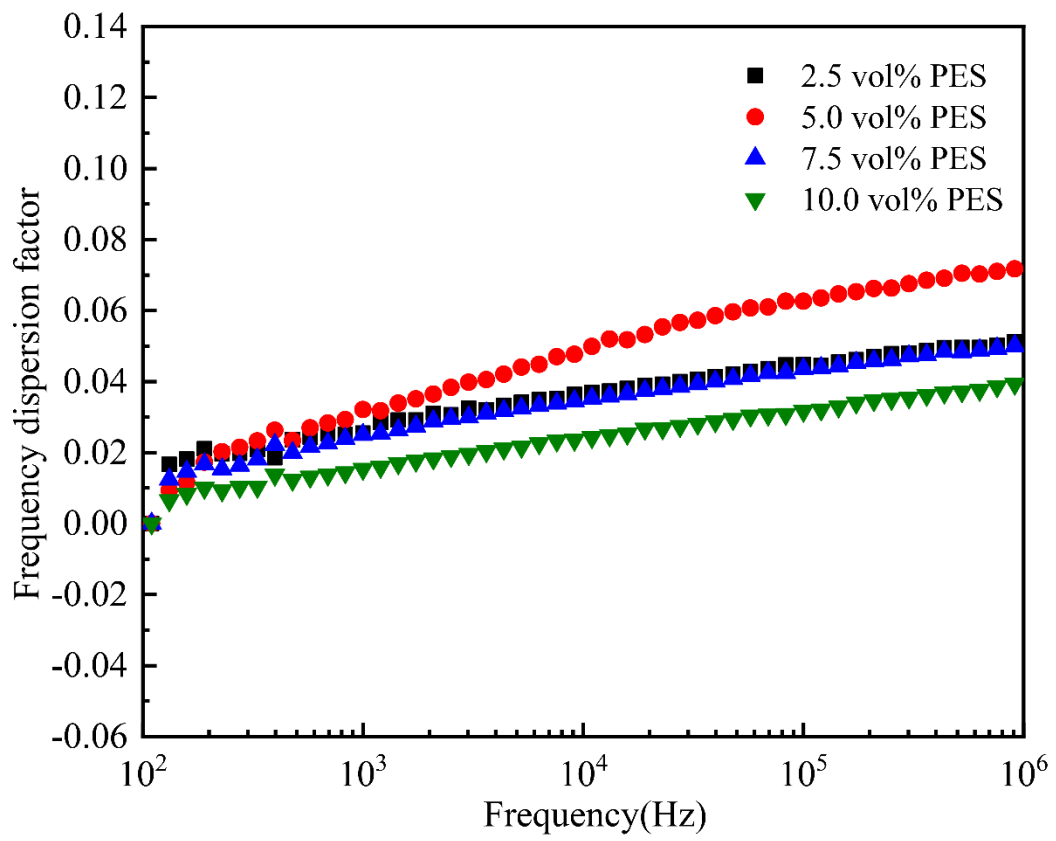


Fig. 7 The frequency dispersion factor of PES-BST/PEEK composites.

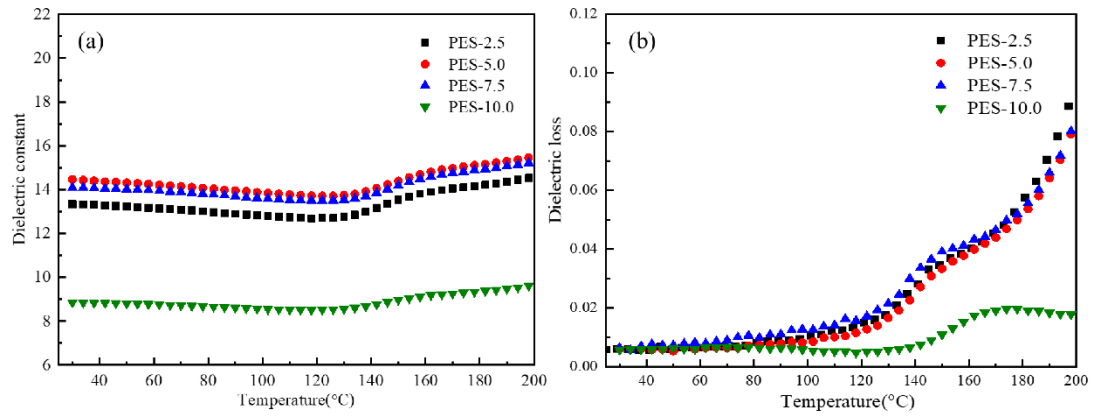


Fig. 8 Temperature dependence of dielectric properties of PES-BST/PEEK composites at 1k Hz, (a) dielectric constant and (b) dielectric loss.

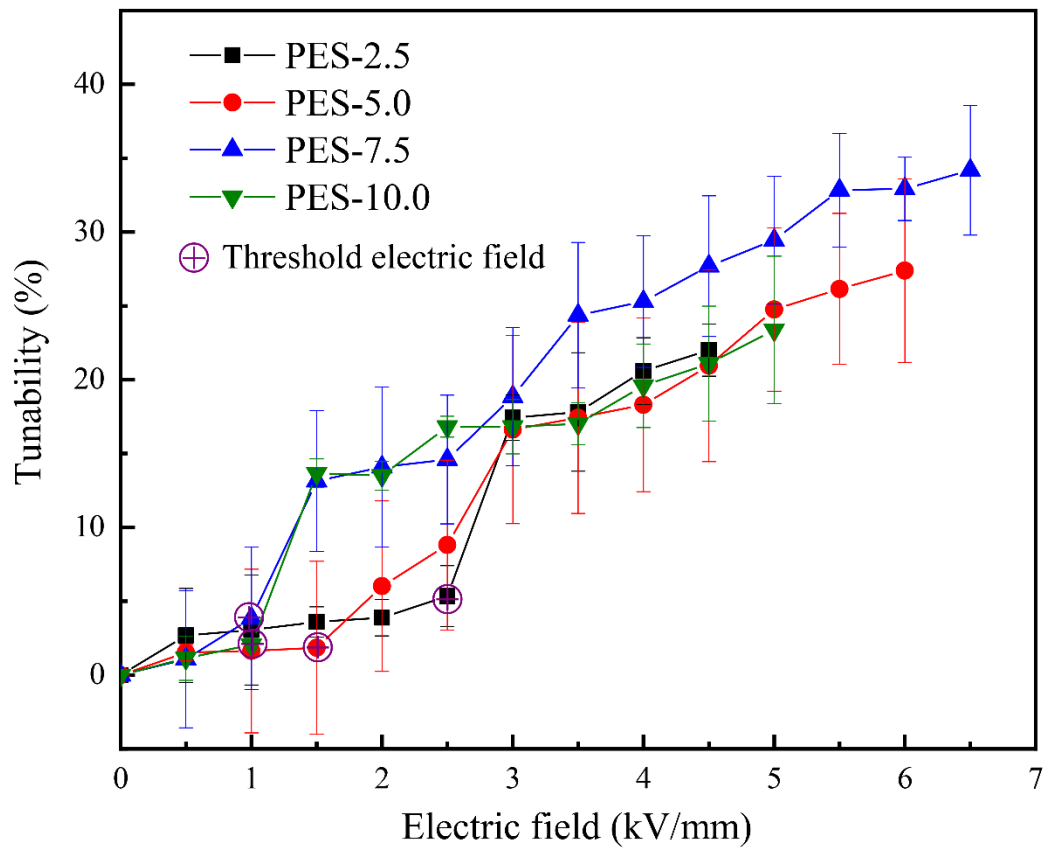


Fig. 9 Dielectric tunability of PES-BST/PEEK composites.

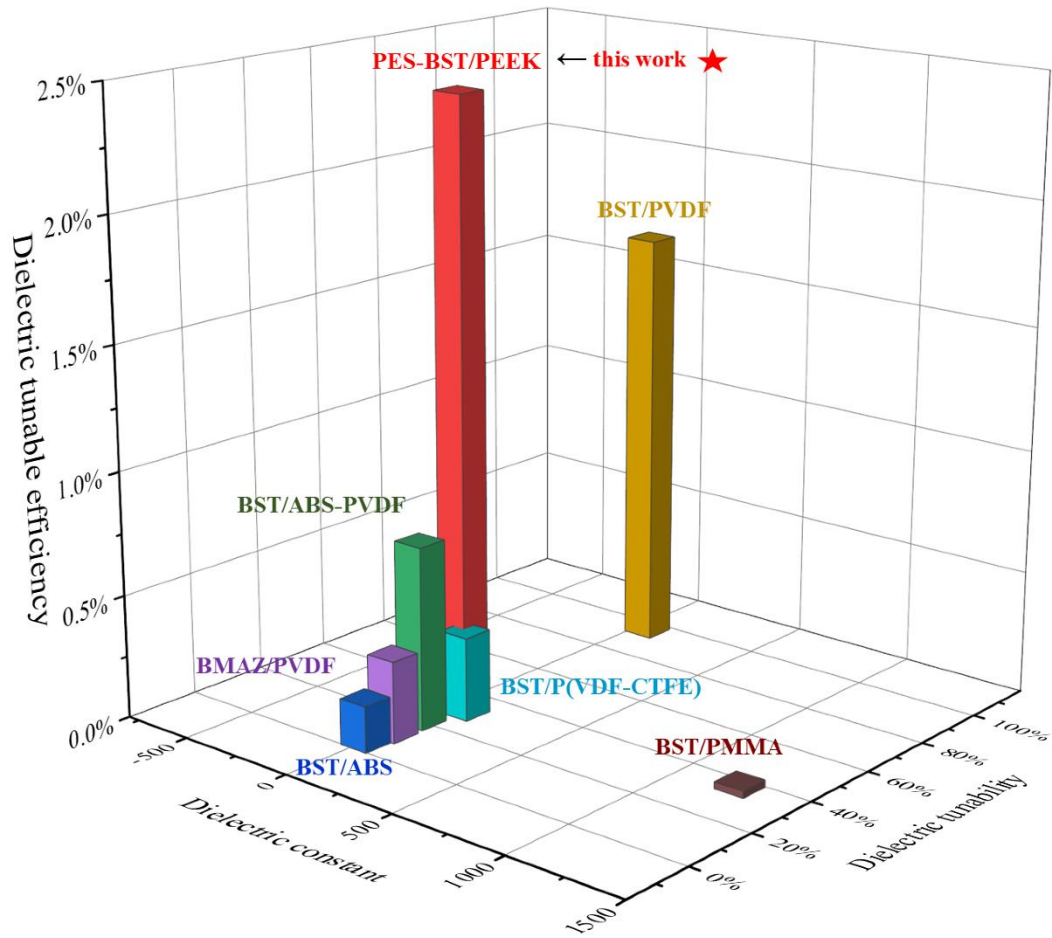


Fig. 10 Dielectric properties of BST/polymer composites.

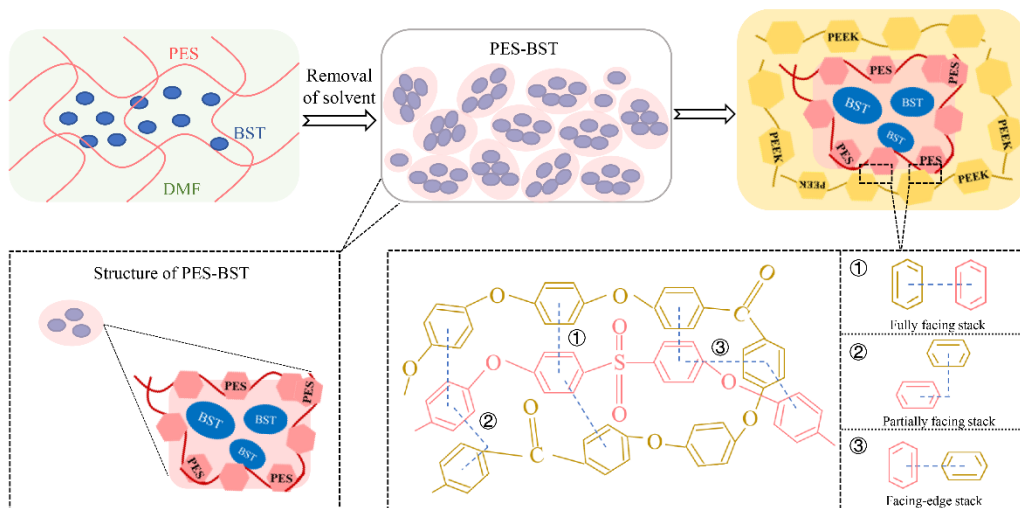


Fig. 11 Modification mechanism of PES-BST/PEEK composites.

Table Captions

Table 1 Composition of PES-BST/PEEK composites

Table 2 Glass transition temperature and melting point of PES-BST/PEEK composites

Table 3 Dielectric properties of PES modified BST/PEEK composites

Table 4 Dielectric properties of BST/polymer composites

Table 1 Composition of PES-BST/PEEK composites

Sample label	BST content (vol%)	PES content (vol%)	PEEK content (vol%)
PES-2.5	40	2.5	57.5
PES-5.0	40	5.0	55.0
PES-7.5	40	7.5	52.5
PES-10.0	40	10.0	50.0

Table 2 Glass transition temperature and melting point of PES-BST/PEEK composites

Samples	BST/PEEK	PES-2.5	PES-5.0	PES-7.5	PES-10.0
Density (g/cm ³)	2.35	2.494	2.511	2.525	2.568
Glass transition temperature (°C)	144.3	154.8	159.1	160.4	162.6
Melting point (°C)	344.5	332.7	322.5	328.6	312.6

Table 3 Dielectric properties of PES modified BST/PEEK composites

Material composition	BST/PEEK	PES-2.5	PES-5.0	PES-7.5	PES-10.0
Dielectric constant (1kHz)	13.3	13.5	15.0	14.2	8.9
Dielectric loss (1kHz)	0.017	0.007	0.016	0.009	0.006
Frequency dispersion factor (1M Hz)	0.065	0.051	0.072	0.051	0.04
Threshold electric field (kV/mm)	2.0	2.5	1.5	1.0	1.0
Dielectric tunability (%)	8.75	22.00	27.38	34.18	23.37
Breakdown strength (kV/mm)	11.15	28.45	38.02	41.37	36.18

Table 4 Dielectric properties of BST/polymer composites

Composites	Ceramic content/vol%	$\epsilon_r@1$ kHz	$\tan\delta@1$ kHz	$F_{(IM)}$	T_u (%)	T_{uE} (%)	Reference
BST/ABS	40	18	0.082	0.318	3.36	0.187	[19]
BST/ABS-PVDF	40	27	0.090	0.364	20	0.741	[21]
BMAZ/PVDF	40	33	0.025	0.061	10.9	0.330	[39]
BST/PVDF	40	56	0.118	0.348	95.2	1.700	[34]
BST/PMMA	41.6	1250	0.020	~0.1	36	0.029	[20]
BST/P(VDF-CTFE)	40	88	0.056	0.773	30	0.341	[40]
PES-BST/PEEK	40	14	0.009	0.051	34.18	2.441	this work